Program Digest, 2019 IEEE International Ultrasonics Symposium (IUS)
Glasgow, Scotland, October 6-9, 2019

A High Power Circuit Model of an FBAR Resonator for Use in Filter Design

Sormeh Setoodeh, Utku Kemiktarak, Farhad Bayatpur, Siamak Fouladi, David Feld
Wireless Semiconductor Division
Broadcom Inc.
San Jose, USA

***Abstract*—FBAR resonators comprise a thin film metal-piezoelectric-metal membrane with an air cavity on either side. Under high power operation an FBAR resonator generates heat which flows within the membrane producing a radial temperature distribution (the highest temperature being in the central region). A high power electro-thermal model must incorporate this radial temperature distribution so that it can adequately capture a resonator's electrical behavior including hysteresis. Prior electro-thermal models, which have been used to model the high-power performance of solidly mounted BAW resonators, assume a uniform radial temperature distribution of the membrane, and are thus incompatible for use in modeling FBAR resonators.**

Keywords—FBAR; thermal; high power; piezoelectric resonator; radial temperature gradient

I. INTRODUCTION

Each new generation of handset must operate over an increasing number of frequency bands. The latest 2-way and 4-way multiple input, multiple output (MIMO) standards require the operation of multiple transmit/receive chains to maximize a handset receive sensitivity and to increase Tx/Rx data rates. The aforementioned evolution in handset design has necessitated an increase in the number of antenna filters in the RF section of a handset's front-end. To keep the RF section small, the footprint of the individual RF components, including the filters must be reduced. At the same time the transmit filters in the RF front-end must pass signals at increasing power levels e.g. high power user equipment (HPUE) standards and thus the filters must operate at higher power densities. FBAR resonator technology, being compact, having a high quality factor, and able to operate at high energy densities is a filter technology of choice. But the power density requirements have become so imposing that transmit filters must be designed with high power operation as a key consideration. A high power circuit model of an FBAR resonator is developed for this purpose.

Prior electro-thermal circuit models were developed for modeling solidly mounted resonator (SMR) technology [1-4]. Since the heat in an SMR resonator is extracted from underneath the resonator through the resonator's Bragg stack, the SMR model assumes that the temperature across the radius of a resonator is uniform. Such a model is incompatible for use in modeling FBAR resonators whose heat is primarily extracted laterally through the membrane, thus producing a strong radial temperature dependence.

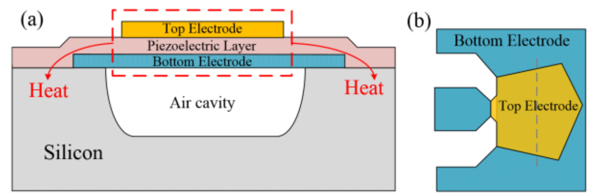

Fig. 1. Cross section (a) and top view (b) of an FBAR resonator

The work described herein is in response to the need for a steady state electro-thermal circuit model which captures a membrane's radial temperature dependence and which as a result is able to accurately model the electrical response of an FBAR resonator operated at high power. By simulating an entire filter design comprising such models, a filter designer can model the steady state strain, electric field, and temperature of each resonator in a filter as a function of the power and frequency applied to the filter's input. She can also use the model to optimize the filter's response in the presence of a high power tone.

Prior electro-thermal FEM models of an FBAR resonator have been constructed [5-7] which incorporate both the 3D thermal physics of an arbitrarily shaped resonator and a resonator's 1D electro-mechanical behavior. Such models are intended for simulating the electro-thermal response of a filter design with a given layout. The advantage of such an approach is that the precise 3D shape of each resonator is factored into simulation. But during the prototyping phase of a filter design, having to layout numerous filter designs with arbitrary resonator topologies to be considered is cumbersome. Therefore, a flexible electro-thermal model of a resonator which crudely accounts for the different shapes of the various resonators in a filter design is needed. A designer can use this high power circuit model in conjunction with small signal RF and nonlinear models to optimize and tradeoff between the various requirements of her filter design.

In both the FEM and circuit modeling approaches, lateral mode physics is neglected because it is too computationally intensive to implement. As a result, the lateral mode physics must be phenomenologically incorporated back into these models to adequately compensate for the missing physics. To this end our circuit model employs a careful balance between physics and phenomenology, and as will be described later, the phenomenological parameters are tuned such that our model is in tight agreement with measured resonators in a given layer stack. This enables higher accuracy predictions when modeling a filter comprising such resonators.

II. HIGH LEVEL DESCRIPTION OF HIGH POWER ELECTRO-THERMAL RESONATOR MODEL

A piezoelectric FBAR resonator comprises a freestanding thin film metal-piezoelectric-metal membrane sandwiched between two air cavities which is anchored to a Silicon substrate at the membrane's perimeter, Fig. 1a. The resonator is patterned into a convex polygon as shown in Fig. 1b. When such a resonator is driven at its resonant frequency, thickness extensional mode vibrations are excited within the membrane. The air cavities on either side of the membrane act as acoustic reflectors, with negligible acoustic energy leakage at the membrane/air interfaces and enabling the resonator to have a high quality factor.

The air cavities also confine the heat which is generated by electrical and mechanical dissipation in the interior of the membrane to flow laterally through the membrane outward from the central region resulting in a radial temperature gradient across the membrane with the central region of the resonator being the hottest, and the perimeter of the resonator being the coldest.

Fig. 2 shows a typical measured small signal RF response (Z_{11}, S_{11}) of an FBAR resonator in blue, and the small signal RF response in the presence of a high power tone in red (the hot S parameter response). Self-heating of the resonator by the high power tone shifts the Z_{11} response to a lower frequency. In addition, a small loop is formed on the Smith chart in the vicinity of the resonant frequency (fs). This loop results from the fact that there is a radial gradient in the resonant frequency of the membrane which is in turn a result of the aforementioned temperature gradient across the radius of the membrane (IR measurement of a resonator shown in the figure). Such a loop phenomenon can be modeled by dividing the resonator up into two or more sections having slightly different resonant frequencies which are electrically in parallel with one another [8]. Such a circuit model: (1) mimics the observed loop in its small signal response as the power level of the high power tone is increased, and (2) gives rise to the observed hysteretic response in the resonant frequency when the high power tone is stepped across a range of frequencies in the vicinity of the loop (to be described in section IV).

In order to maximize the quality factor, an FBAR resonator is typically laid out as a convex polygon. For purposes of thermal modeling, such a resonator is approximated as a circular disk. If the metal electrodes are sufficiently thick, it is reasonable to assume that the disk receives uniform electrical excitation throughout its volume. As a result, the temperature, electric field, and strain distributions will be independent of azimuth and dependent only on radial position. The disk can be subdivided

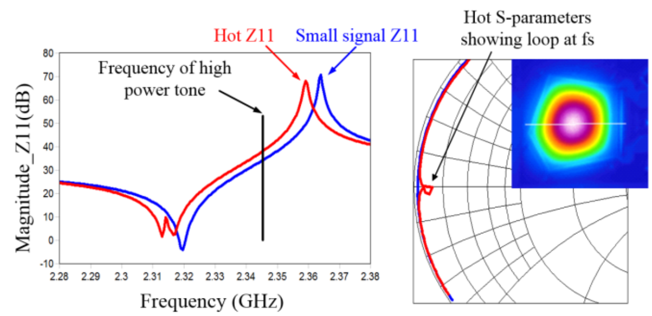

Fig. 2. Measured s-parameters of a resonator in the absence of a high power tone (blue) and in the presence of a high power tone applied to peak of group delay (red). Red trace shows the formation of a loop near the resonance frequency due to the strong temperature gradient across the resonator.

into a set of concentric annular rings as is shown in Fig. 5b. We assume that each ring is isothermal (having a constant temperature throughout its volume), with the innermost/outermost rings being the hottest/coldest rings respectively. And because each ring is at a uniform temperature, its electrical, mechanical, and thermal behavior can be lumped together, and the set of rings can then be modeled as a linear array of interconnected lumped models. We should note that in practice resonators will have arbitrary polygonal shapes and will thus be non circular. However, our basic assumption of 1D heat flow from the central region to the edge of the resonator is still valid and we can always find a set of isothermal contours which are not necessarily circular.

Each ring is modeled as a single lumped Mason model whose material parameters -- e.g. the electrical resistance of the metals and the bulk modulus of the piezoelectric layer -- are functions of the (isothermal) temperature of the ring[1]. We note that each Mason circuit has two electrical ports and two mechanical ports corresponding to the upper/lower electrodes of each ring. We have extended the Mason circuit to include a single thermal port to which heat can enter/leave the ring. As is standard practice both the electrical and mechanical behavior of the Mason circuit are modeled as an electrical circuit. We have included the thermal behavior in the Mason circuit such that the electrical, mechanical, and thermal behavior of each ring is modeled entirely as an electrical circuit. We note that lateral mechanical coupling between adjacent rings which is impractical to implement in a circuit model, is neglected.

III. CONSTRUCTION OF A HIGH POWER RESONATOR MODEL COMPRISING THERMAL MASON CIRCUITS

First we discuss the construction of a thermal Mason circuit corresponding to a single ring and then show how a set of such circuits can be connected together to form a high power model of a resonator. Modeling of the thermal Mason circuit requires a thermal model of the piezoelectric and metal layers comprising the ring. Both the thermal coefficient of expansion (TCE) and the thermal coefficient of the bulk modulus (TCB) of the films give rise to a resonator's thermal coefficient of

[1] Examples of temperature dependent materials constants are: (1) the bulk modulus of the metal films, and (2) the bulk modulus, dielectric constant, and piezoelectric constant of the piezoelectric layer.

frequency (TCF). However, as shown by Larson [9] the TCB is by far the dominant term, and hence we assume that the TCF of a resonator is entirely a consequence of the TCB's of the piezoelectric and metal films.

The piezoelectric layer is modeled by employing the following constitutive relations:

$$T = c^D S - e\frac{D}{\varepsilon^S}$$

$$E = \frac{D - eS}{\varepsilon^S}$$

We incorporate the temperature dependence of the bulk modulus (TCB) for the piezo layer as follows:

$c^D(\Delta\theta) = c^D(1 + \alpha\Delta\theta)$ where $\alpha = 2 \times TCF$

where $\Delta\theta$ is temperature rise and $\alpha = 2 \times TCF$. TCF is assumed to be -26ppm/°C for the AlN layer.

A temperature dependent stress/strain equation is arrived at by substituting the temperature dependence of the bulk modulus into the stress/strain constitutive equation as follows:

$$T(\Delta\theta) = c^D S - e\frac{D}{\varepsilon^S} + (c^D S\alpha\Delta\theta)$$

Similarly, we include the temperature dependence of the metal electrodes into their stress/strain constitutive equation using TCF = -50ppm/°C for the Molybdenum layer [9].

The aforementioned temperature dependent constitutive equations for the metal and piezoelectric films are implemented into a single section "thermal" Mason model as shown in Fig. 3. The temperature dependent voltage sources, which are proportional to the temperature rise ($\Delta\theta$) of the films effectively vary the bulk moduli of the metal and piezoelectric films respectively.

Next we couple a set of individual thermal Mason models (representing rings) together to form a high power model of a resonator as shown in Fig. 4. The heat flow that is generated by each ring due to dissipation in its corresponding Mason model (discussed in further detail in section IV) is represented by a dc current source whose amplitude is the total heat dissipation rate within the ring. The current sources (heat flow sources) from adjacent rings are coupled together through lumped thermal resistors (electrical series resistors between adjacent rings), as is shown in the figure. The temperature rise of each ring, represented by the node voltage at the top of each current source, is fed into the thermal port of its respective Mason model varying the temperature dependent materials parameters linearly. We use a physical model described in appendix I to calculate the thermal resistances used in our model.

Since the rings share a common upper/lower electrode, the corresponding upper/lower electrical terminals of each ring's Mason model are wired together in parallel, while the two mechanical ports of each Mason model are grounded (representing the high acoustic impedance of the air above/below each ring), as is shown in Fig. 3.

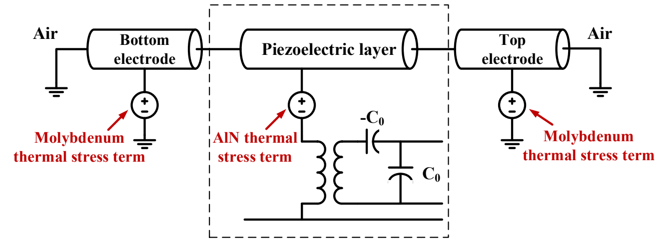

Fig. 3. Schematic of a temperature dependent Mason model

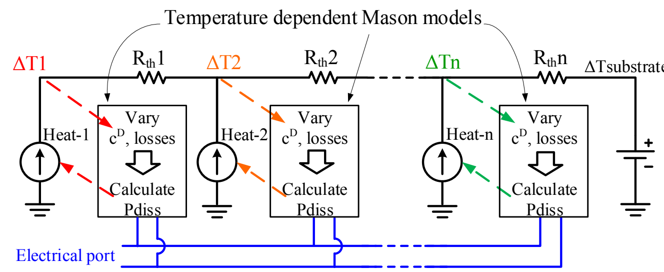

Fig. 4. Block diagram of a multi-section electro-thermal circuit model for an FBAR resonator

Standard modeling methods suggest that subdividing the resonator into a larger number of isothermal sections will produce a more accurate simulation result. However, because we have chosen to neglect lateral mode physics, a larger number of sections does not necessarily produce higher modeling accuracy. Needless to say, there is a tradeoff between the number of sections and the simulation time.

The state variables of the entire electro-mechanical thermal model of the resonator, being a collection of nonlinear electrical circuit elements, can under the influence of an applied high-power electrical stimulus, be solved by a nonlinear circuit solver such as Keysight's harmonic balance solver [10]. In addition, the state variables of a collection of such resonators comprising a filter can be solved using such a solver.

IV. Empirical Extraction of the High Power Circuit Model Parameters

The small and large signal behavior of a given resonator is characterized and used to generate a high power model of the same.

We start with our standard Mason model, which incorporates three resistors representing the ohmic, mechanical, and dielectric losses of a resonator. The values of the three resistors are adjusted to fit the measured small signal S parameters of a resonator. To capture the temperature dependence of each of the three resistors -- the lower Q of the resonator at higher temperatures -- temperature coefficient variables are incorporated into our model.

We also note that only a portion of the dissipated power in the resonator -- dissipated by the 3 aforementioned resistors -- will be converted into heat inside of the active region. We use three heat conversion factors (HSF) to account for the fraction of the dissipated power in each resistor which is converted into heat.

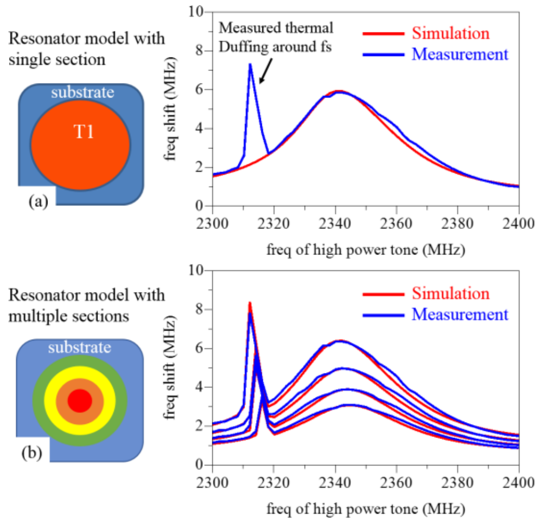

Fig. 5. Simulated frequency shift vs. frequency of high power tone for an FBAR resonator at high power assuming: (a) uniform temperature across the resonator (1 power level shown) and (b) multiple sections with different temperatures capable of modeling the measured thermal Duffing effect at fs (4 different power levels shown).

The aforementioned sets of variables – the three temperature coefficient and three HSF variables – are adjusted such that the measured and modeled frequency shifts of the resonator in the presence of a high power tone are brought into agreement. Fig. 5b shows an example of a frequency shift of a resonator and its corresponding fitted model. Note that hysteresis (thermal Duffing) is exhibited in the measurement in the vicinity of the resonant frequency, fs. Good agreement is achieved at all frequencies and power levels. For reference we also show a fit of our data to a single section model (Fig. 5a) showing that the hysteretic behavior cannot be captured.

I. Using the High Power Circuit Model to Predict the High Power Repsonse of a Filter

One of the advantages of the present electro-thermal circuit model is that a designer can use it in the same ADS environment where she optimizes her filter design to meet the RF and nonlinear specifications. The high power response of a filter design as the topology and areas/frequencies of the resonators are modified to span a design space, can be understood without having to layout each new filter topology and switch back and forth between a circuit simulator an FEM solver.

When the thermal Mason model for a resonator is calibrated for a given stack, it can be used to simulate the high power response of any filter topology accurately. Fig. 6 shows an example of simulated (blue) vs. measured (red) hot s-parameters for a filter design for a given incident power level.

The thermal parameters for this stack were tuned by fitting the electro-thermal model to 5 different resonator areas within the same stack. The filter is measured on wafer without its matching elements. Each trace shows the hot s-parameter of the filter at a specific stress frequency point.

This model is also used to predict the high power response of a filter in a module by incorporating the thermal resistance and s-parameters of the module.

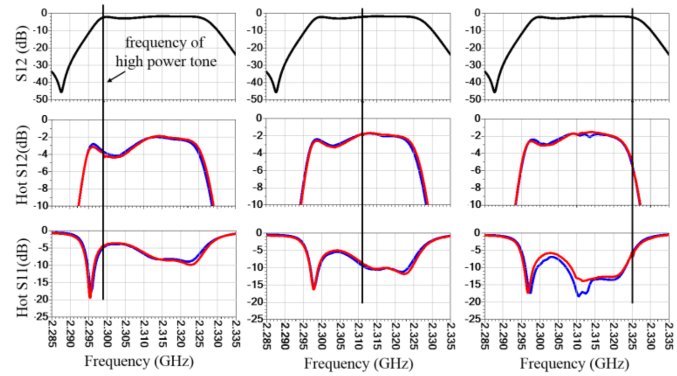

Fig. 6. Measured S12 of a filter before applying high power tone (black) and its simulated (blue) vs. measured (red) hot s-parameters in presence of a high power tone at 3 frequency points at low, mid and high channel shown on left middle and right columns. Incident power is held constant.

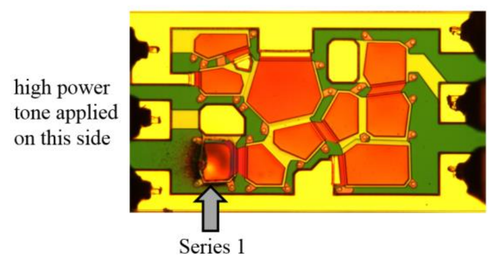

Fig. 7. Photomicrograph of a failed filter after an excessively high power tone was applied to the filter's input. The frequency of the applied high power tone corresponded to the filter's high frequency corner. The model predicted that the failed series-1 resonator (shown) would fail first. It also closely predicted the incident power level at which the resonator failed.

For any given filter at an arbitrary input frequency, there is a certain maximum power level that the filter can withstand prior to irreversible damage. The failure is generally confined to a single resonator within the filter. For any given frequency one can determine the resonator most likely to fail first, and the corresponding input failure power level. As an example we used our model to identify for a high channel Tx input signal that the weakest resonator was series-1 as shown in Fig. 7, and we also determined the failure power of the filter within 0.5 dB.

II. Summary

A high power circuit model of an FBAR resonator was developed for use in a filter's prototyping phase capturing a resonator's radial temperature distribution. The model predicts the large signal and hot S parameter responses of an FBAR resonator at all frequencies including hysteresis behavior (Duffing effect) in the vicinity of the resonant frequency. While each section of the circuit model is based on a 1D Mason model modified to include thermal effects, a set of phenomenological parameters allows the model to be precisely tuned to high power measurements of an FBAR process comprising arbitrary materials and layer stack thicknesses. The model was used to predict a filter's hot and large signal S parameters when a high power tone stimulus -- with an arbitrary frequency and power level -- is applied to the filter's input. The model was also used to identify the weakest resonator in a filter, e.g. the first resonator to fail as the filter's input power is increased.

III. APPENDIX – I

In this section we discuss: (1) selection of the thermal resistances when a finite number of annular rings is used and (2) how to incorporate thermal resistance for higher aspect ratio resonators.

We calculate the thermal properties of a resonator as a central circular disk and finite number of concentric rings surrounding that disk. In this model, the heat generated in the membrane runs from the hot central disk, through the cooler outer rings, to the cold substrate at the perimeter, reducing the thermal problem down to one dimension.

We develop a lumped circuit model that represents the thermal properties of the, as shown in Fig. 8. We calculate the thermal resistances by assuming that, in each section the heat is generated uniformly at a constant rate. This allows us to calculate a temperature profile for that section, given the boundary conditions. Then the temperature profile and the model leads to a thermal resistance network for that section.

We model the thermal properties of each ring using two separate thermal resistances (Fig. 8): One for the heat that is generated in a section which is closer to the middle of the membrane, and a second one for the heat that is generated within that ring. This approach models the thermal properties of a circular membrane more accurately in the limit of a small number of rings, compared to a model which ignores the source of the heat and uses a single thermal resistance per ring. In the limit where the number of rings goes to infinity these two models are equivalent.

We solve the heat equation [11] for a ring with the relevant boundary conditions to get:

$$R_{ext} = \frac{ln(r_2/r_1)}{2\pi dk} \tag{A1}$$

and:

$$R_{in} = \frac{1}{4kd}\left(1 - \frac{2\,ln(r_2/r_1)}{r_2^2/r_1^2 - 1}\right) \tag{A2}$$

We use the same method to calculate the thermal resistance, R_d, of the central disk:

$$R_d = \frac{1}{4kd} \tag{A3}$$

Once we calculate all thermal resistances in the model, series pairs of resistances shown in Fig. 8 between each current (heat) source can be combined to achieve one thermal resistance per section, as shown in Fig. 4.

It is well known that electrical and thermal parameters of thin films for example can be very different from their bulk values and very sensitive to the fabrication process [12]. In this work we use the values of the thermal conductivities (k) for the piezoelectric and metal films from thin film measurements. Any errors in these material values are compensated for by the fitting procedure described in section IV.

A resonator's aspect ratio has the largest impact in determining the thermal resistances of each section in an FBAR resonator, and therefore aspect ratio must be included as a parameter in the model. A look up table for different aspect ratios is generated to scale the set of thermal resistances calculated for the circular resonator. The values of this lookup table can be determined from 3D thermal simulations or hot S parameter measurements of resonators with different aspect ratios.

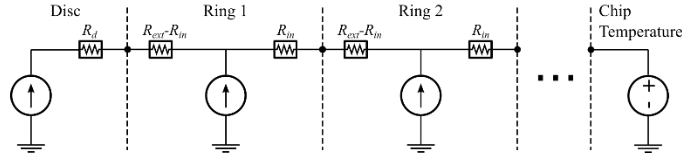

Fig. 8. Thermal model of each section described by two thermal resistances and a current (heat) source. The substrate temperature on the right is modeled as a voltage source.

ACKNOWLEDGEMENTS

The authors thank Genichi Tsuzuki for fruitful discussions in inspiring this work. We also thank Brice Ivira for providing IR pictures of resonator at high power.

REFERENCES

[1] J.Rosenbaum, "Bulk Acoustic Wave Theory and Devices", Artech House.
[2] A. Tag et al., "Multiphysics Modeling of BAW Filters," 2015 IEEE International Ultrasonics Symposium (IUS), Taipei, 2015, pp. 1-4.
[3] A. Tag et al., "Effect of spatial distribution of dissipated power on modeling of SMR BAW resonators at high power levels," in IEEE Transactions on Ultrasonics, Ferroelectrics, and Frequency Control, vol. 62, no. 10, pp. 1856-1864, October 2015.
[4] M. Fattinger, P. Stokes and G. Fattinger, "Thermal modeling of WLP-BAW filters: Power handling and miniaturization," 2015 IEEE International Ultrasonics Symposium (IUS), Taipei, 2015, pp. 1-4.
[5] C. Kirkendall and B. Ivira, "A Hybrid 3D Thermal / 1D Piezoelectric Finite Element Model for Rapid Simulation of FBAR Filter Response Under High Power," 2018 IEEE International Ultrasonics Symposium (IUS), Kobe, 2018, pp. 1-6.
[6] B. Ivira and C. Kirkendall, L Lipiannen, "Transient response of BAW resonators," in Proc. IEEE Int. Ultrasonics Symp., Oct. 2019.
[7] Jeff Tharp, ANSYS, Private communication. March 2018
[8] D. A. Feld, S. Fouladi, P. Bradley, J. Larson and R. Ruby, "Unbalanced device comprised of FBAR resonators," 2012 IEEE International Ultrasonics Symposium, Dresden, 2012, pp. 71-76.
[9] J. D. Larson and Y. Oshrnyansky, "Measurement of effective kt^2, q, Rp, Rs vs. Temperature for Mo/AlN FBAR resonators," 2002 IEEE Ultrasonics Symposium, 2002. Proceedings., Munich, Germany, 2002, pp. 939-943 vol.1.
[10] Agilent Technoogies Advanced Design System harmonic balance
[11] Incropera, DeWitt, " Fundamentals of Heat and Mass Transfer", Wiley.
[12] Bogner, Manuel, Benstetter, Günther and Fu, Yong Qing (2017) Cross- and in-plane thermal conductivity of AlN thin films measured using differential 3-omega method. Surface and Coatings Technology, 320. pp. 91-96. ISSN 0257-8972